Next Materials 8 (2025) 100723

Contents lists available at ScienceDirect

Next Materials

journal homepage: www.sciencedirect.com/journal/next-materials

Research article

Development of tertiary butyl hydroquinone based polybenzoxazine for effective anti-microbial and anti-corrosion coating applications

Hariharan Arumugam [a,*], Harinei Srinivasan [b], Mohanapriya S.N [b], Alagar Muthukaruppan [b,c]

[a] Department of Chemistry, Arumugam Pillai Seethai Ammal College, Tiruppattur, Tamil Nadu 630211, India
[b] Polymer Engineering Laboratory, PSG Institute of Technology and Applied Research, Neelambur, Coimbatore 641 062, India
[c] Centre for Advanced Materials, PSG College of Arts & Science, Coimbatore 641014, India

ARTICLE INFO

Keywords:
Tertiary butyl hydroquionone
Polybenzoxazine
Anticorrosion coatings
Thermal stability
Antimicrobial activity

ABSTRACT

The work presents a new type of polybenzoxazines synthesised using tertiary butyl hydroquinone (THQ) with aromatic and fluorinated mono functional amines such as aniline (a), ethynylaniline (ea), cyanoaniline (ca), fluoroaniline (fa), trifluoromethylaniline (tfma) and 4-fluorotrifluoromethylaniline (4ftma). The structure of the benzoxazines were elucidated using spectroscopyic technique. The curing behaviour, thermal stability of the THQ polybenzoxazines were studied in order to assess their performance in high themperature environments. Among the six polybenzoxazines synthesized, the tert-butyl hydroquinone with cyanoaniline based polybenzoxazine shows the exceptional thermal stability with higher residual value of 60 % and higher degradation temperature of 553 °C. The moisture resistance behaviour of the synthesized THQ polybenzoxazines have been studied and all the THQ polybenzoxazines possess excellent hydrophobicity. The synthesized THQ polybenzoxazines were tested for their surface protection efficiency as anti-corrosive coatings on mild steel surfaces. The poly(THQ-4ftma) polybenzoxazine coating exhibits excellent corrosion resistant behaviour with efficiency of 99.99 %. All the six THQ polybenzoxazine coated mild steel specimen shows better corrosion resistant behaviour than that of the uncoated mild steel. In addition to the above, THQ benzoxazines were checked for their antibacterial activity (against *S. aureus* and *E.coli*) was checked and inhibition zone was observed at greater than 25 mm. The results obtained from different studies indicate that the tert-butyl hydroquinone based benzoxazines can be effectively used as a multifunctional coatings under high thermal environment and protection against microbes including adverse corrosive environment.

1. Introduction

Protection of mild steel surfaces from corrosion is one of the important practices used in wide range of industries to safeguard mild steel structures and machineries. Various types of materials have been used as coating material to protect the metallic surfaces from corrosion [1,2], however, the stability and efficiency of the coatings were still a permanent challenge for researchers, and the industries. The coating of materials principally consist of a polymeric binder capable of forming adherent film over the metallic substrates. Varied nature of polymeric materials have been utilized as the binder such as epoxy resins, polyurethane resins, alkyd resins, inorganic resins, vinyl resins for the preparation of coatings to protect the surfaces from corrosion [3,4]. Some of these thermosetting binders require external thermal energy for the polymerization process. In addition to the binder, the anti-corrosive pigments such as salts of zinc, aluminium, titanium, etc are added to the coating formulation, which plays the major role in acting as a barrier [5,6]. Hence, researchers are interested to develop a polymeric material which can perform both as binder as well as anticorrosive material.

One such material is polybenzoxazines, which is a versatile material possessing excellent thermal stability along with good hydrophobicity [7,8]. The benzoxazine monomers does not require an external curing chemical agents, but it requires thermal energy to gets cured/polymerized. Nowadays, several reports have been found on using the polybenzoxazines as an effective anti-corrosion coating [9–11]. For instance, Deng et al., synthesized curcumin based benzoxazine for anti-corrosion and anti-fouling applications. Their results showed that the polybenzoxazine coated substrates showed excellent corrosion

* Corresponding author.
E-mail address: hariharannalan@gmail.com (H. Arumugam).

https://doi.org/10.1016/j.nxmate.2025.100723
Received 6 February 2025; Received in revised form 7 May 2025; Accepted 13 May 2025
Available online 16 May 2025

resistance and their anti-fouling behavior enhanced when PEG was added to the coating. They also studied the performance of double coating with another layer PEG mixed polybenzoxazine and the results are further improved [12]. Zhou et al., prepared a novel silane functionalized polybenzoxazine anti-corrosion coating with better adhesion to the stainless steel [13]. An interesting study has been reported by Wang and team that deals with the fabrication of a superhydrophobic and anti-corrosion coating using polybenzoxazine composite with hexagonal boron nitride. They achieved a water contact angle value of 158.2° for the superhydrophobic coating [14]. Most of the study reports the development of anti-crrosion coating by blending polybenzoxazine with some superhydrophobic or adhesion enhancing agents[15–17]. Another study from Ahmed M. M. Soliman et al., reports the development of salicaldehyde with n-hexylamine benzoxazine coating and achieved a corrosion protection efficiency of 91.7 % for the polybenzoxazine coating itself without adding any external superhydrophobic or adhesion enhancing agents [18].

Another important problem in marine environment is the attack of microbes over the metal surface which leads to fouling of the material [12,19]. There are several works carried out to protect the material's surface from microbial attack, but some of them lacks the property of anti-corrsion behavior. The conventional inorganic anti-microbial coatings require tedious processing to bind over the materials surface [20,21]. Polybenzoxazines are less explored in the area of anti-microbial resistance. Very limited novel works of using polybenzoxazine as anti-microbial agent has been reported in the literature. For instance, CJ raorane reported the synthesis of curcumin/aniline benzoxazine and developed a antibiofilm against *C.Albicans*, which also exhibits more than 90 % corrosion protection efficiency [22]. T Periyasamy reports the development of curcumin-furfurylamine polybenzoxazine, which is blended with chitosan to form a effective anti-bacterial film [23]. Sahu et al. reports the synthesis of vanillin/disulfide containing amine based benzoxazine and developed biofilms using the synthesized benzoxazine-grafted-chitosan. The biofilms achieved excellent bactericidal properties of approximately 99 % against both *E. coli* and *S. aureus* bacteria [24]. However, polybenzoxazine alone which can act as both anti-corrosive and anti-bacterial material is warranted.

Various phenolic and amino compounds were used to synthesis the benzoxazine resins. Tert-butyl hydroquinone is a phenolic compound that have good antimicrobial active sites [25–27]. Very few work have been explored in benzoxazine field using Tert-butyl hydroquinone. The fluoro substituted amines and phenolic compounds helps to improve the hydrophobic nature of material [28,29]. Comparitivly, the nitril and acetylene groupsubstituted benzoxazine resins possess better thermal stability than other benzoxazines.

An objective of developing a material which can perform as thermaly stable, hydrophobic, anti-microbial and effective anti-corrosion coating, a new type of polybenzoxazines have been synthesized using tert-butyl hydroquinone (THQ). The THQ benzoxazines were developed using different aromatic amines such as aniline (a), ethynylaniline (ea), cyanoaniline (ca), fluoroaniline (fa), trifluoromethylaniline (tfma) and 4-fluorotrifluoromethylaniline (4ftma) containing aniline core. The developed benzoxazines were studied for their anti-bacterial activity against a gram positive and a gram negative bacteria. The THQ- polybenzoxazines were tested for their efficiency as a barrier against corrosive environment. The hydrophobic behaviour of the synthesized polybenzoxazines were also studied and reported in the present work.

2. Raw materials

Tertiary butyl hydroquinone (THQ) was obtained from Otto chemicals Pvt Ltd. Ethyl acetate and aniline (a) was purchased from Isochem laboratories. Fluoro aniline (fa) was obtained Alfa Aesar chemicals Pvt Ltd. Trifluoromethyl aniline (tfma), and paraformaldehyde were purchased from Sigma Aldrich, India. 4-fluorotrifluoromethylaniline (4ftma), ethynylaniline (ea), and cyanoaniline (ca) were purchased from SRL Chemicals Pvt Ltd. 1,4-dioxane was obtained from Merck Life Science.

3. Experimental

3.1. Synthesis of tert-butyl hydroquinone based benzoxazine resins (THQ-BZ)

Tert-butyl hydroquionone based benzoxazine resines were synthesized using aniline (a) and other five different aniline derivatives such as ethynylaniline (ea), cyanoaniline (ca), fluoroaniline (fa), trifluoromethylaniline (tfma) and 4-fluorotrifluoromethylaniline (4ftma). About 0.02 mol of above mentioned amines were separately mixed with 0.04 mol of paraformaldehyde at ice cold condition in the presence of dioxane solvent. The mixture was kept stirring at room temperature for 30 min and then the temperature was raised to 60 °C. After 1 h of efficient agitation, 0.01 mol of tert-butyl hydroquinone was added to the reaction mixture and the temperature was gradually raised to 110 °C. After the completion of reaction about 4 h, the product resulted was cooled and washed with 2 N NaOH to remove the unreacted compounds. The obtained THQ-BZ monomers were labeled as THQ-a, THQ-ea, THQ-ca, THQ-fa, THQ-tfma and THQ-4ftma (Schemes 1 and 2).

3.2. Preparation of THQ-PBZ

The polymerization of **tert-butyl hydroquinone based polybenzoxazines (**THQ-PBZ) was carried out through a stepwise thermal curing (Scheme 3). The THQ-BZ monomer resins were taken separately in petri plates coated with silane. To remove the excess solvent the samples were heated initially at 70 °C for 8–10 h. Further the temperature was upraised to 110 °C and maintained for 3 h. Then the samples were subjected to stepwise heating at the rate of temperature 30 °C/1 h. For THQ-a, 120 °C-1h, 150°C-1h, 180°C-1h, and 210°C-1h. Finally, the temperature was increased and post cured at 230 °C and this temperature was maintained for 2 h to complete the polymerization process. Similarly, all the benzoxazine resins were post cured separately at appropriate curing temperature (from DSC analysis). The obtained polybenzoxazines (THQ-PBZ) were labeled as poly(THQ-a), poly(THQ-fa), poly(THQ-tfma) poly(THQ-4ftma), poly(THQ-ea) and poly(THQ-ca), for their respective THQ-BZ monomers.

3.3. Preparation of THQ-PBZ coated mild steel specimen

The mild steel (MS) plates having dimensions of 3 × 2×0.2 cm were taken as substrate for the corrosion resistance coating studies of THQ-PBZ. Initially, the surface of the MS plates was polished using sand paper to attain uniform surface. Then the polished MS plates were kept immersed in ethanol and ultra-sonicated for 10 min to remove the impurities, if any present on the surface. The THQ-BZ monomer solutions with a concentration of 1 g/100 ml in THF solvent were prepared. The prepared THQ-BZ monomer solutions were separately coated on the surface of the cleaned MS plates using drop-casting method. The excess solvent was evaporated by placing the coated MS plates at 60 °C for 1 h. After removing the solvent, the THQ-BZ coated MS plates were thermally cured by following the same steps used to cure the monomer samples (Scheme 4). A uniform coating having thickness 0.5 mm has been achieved on the surface of the mild steel plates. The THQ-PBZ coated cured MS plates were further utilized for corrosion resistance studies.

3.4. Assessment of anti-microbial activity

Antimicrobial behaviour of THQ-BZ was studied trough agar well diffusion method using a gram-negative bacterium and a gram-positive bacterium [30,31]. The Escherichia coli (E. coli, ATCC 53868) and Staphylococcus aureus (S. aureus, ATCC 6538) as target bacteria to

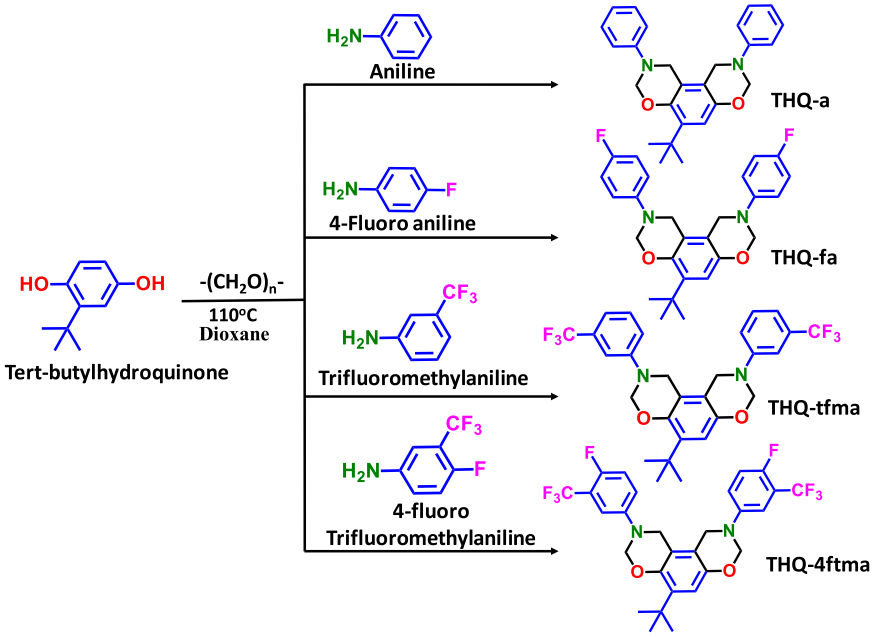

Scheme 1. Synthesis of fluorin substituted THQ-BZ.

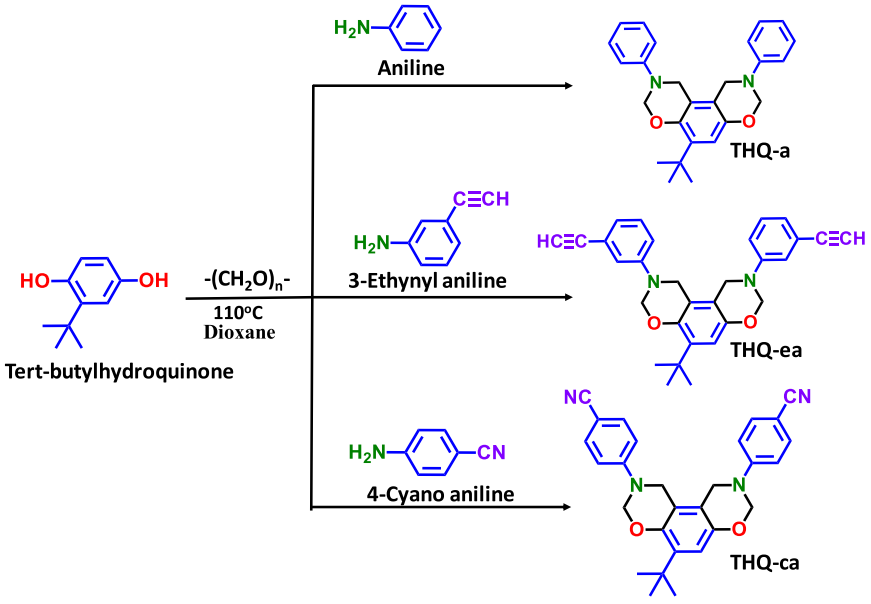

Scheme 2. Synthesis of cyano and ethynyl substituted THQ-BZ.

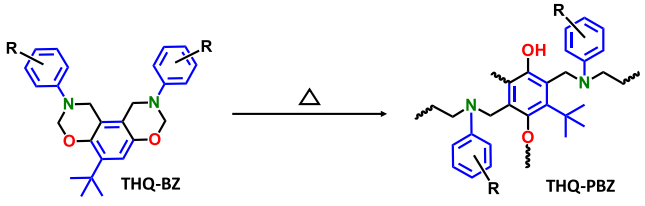

Scheme 3. Preparation of THQ-PBZ.

assess the antibacterial behaviour. The targeted bacterias were developed in nutrient medium. Nutrient agar plates were prepared and the surface of the agar plates were streaked with bacterial isolates using a sterile loop. The plates were kept undisturbed to allow the nutrient agar to solidify and then using a sterile borer, three wells having 5 mm diameter were punched. Further the wells were filled with a standard antibiotic known as ampicillin (A), chloroform (C) as a control and 1 mg/ml of THQ-BZ monomer (Scheme 4). After filling, the culture developed petri plates were incubated for overnight at 37 °C. After that the cultured petri plates were placed for the checking of activity. The zone of inhibitions were measured and discussed.

4. Results and discussion

4.1. Spectral analysis

The formation of oxazine ring in the THQ-BZ monomers were confirmed using proton NMR spectra (Bruker - 400 MHz; Solvent – deuterated chloroform; Standard - tetramethylsilane). The Ar-CH_2-N

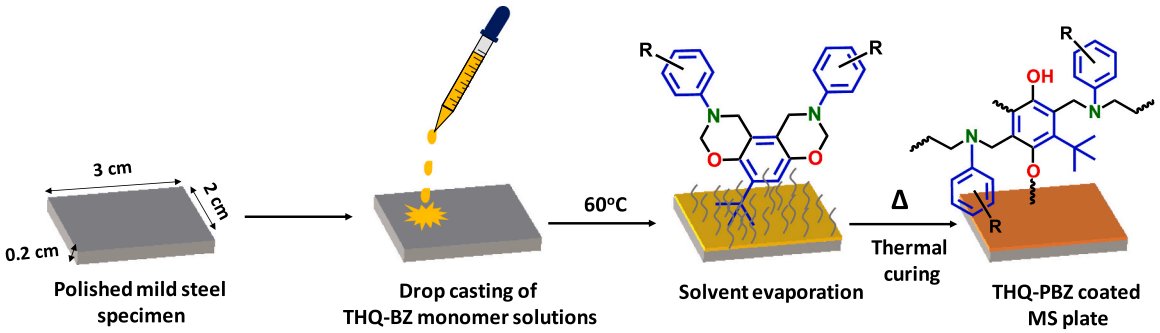

Scheme 4. Preparation of THQ-PBZ coated MS specimen.

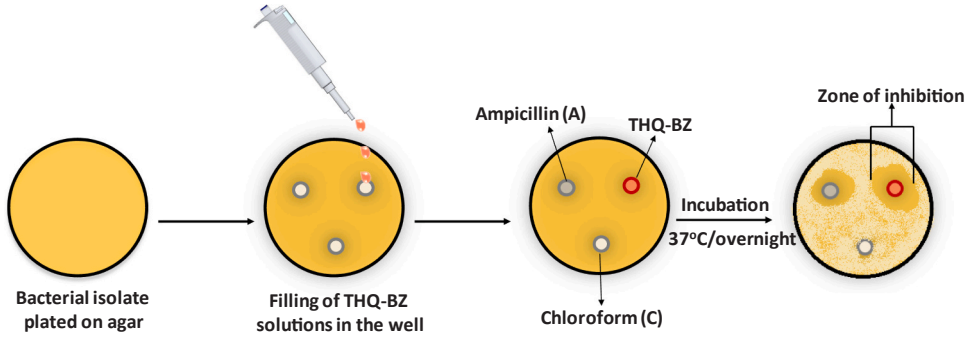

Scheme 5. Representation of agar well diffusion method of THQ-BZ monomers.

proton signal was found at around 4.4 ppm and O-CH_2-N proton signal was found at around 5.3 ppm respectively (Fig. 1). The characteristic oxazine ring signals were appeared as doublets closely situated to one another. This is due to the slight difference in environment of the two oxazine rings. The multiplets appeared around 6.5 – 7.5 ppm in the THQ-BZ monomers infer the presence of aromatic protons. A signal at 1.3 ppm was appeared due to the methyl protons present in tert-butyl group. Fig. 2 represents the ^{13}C NMR spectra of THQ-BZ monomers. The peaks appeared at 48 ppm and 79 ppm corresponds to the Ar-CH_2-N and O-CH_2-N carbons present in the oxazine ring. The signals around 30 and 35 ppm attributes to the tert-butyl group carbons and the peaks appeared between the range of 110–160 ppm corresponds to the aromatic carbons.

From the ^{1}HNMR spectroscopic data, the ring closed ratio (RCR) of THQ based benzoxazines was calculated. The value of RCR of THQ-a, THQ-fa, THQ-tfma, THQ-4ftma, THQ-ea and THQ-ca were obtained at 93 %, 88 %, 84 %, 91 %, 85 % and 96 %, respectivly. The maximum value of RCR provides an identical chemical structure of benzoxazine and physico-chemical properties of polybenzoxazines [32].

The functional groups of THQ based benzoxazine resins were identified using FTIR analysis (ATR-FTIR; Shimadzu IRSpirit spectrophotometer). The characteristic out of plane stretching vibration of oxazine ring was found at 942 cm^{-1} (Fig. 3a). The symmetric and asymmetric stretching of aromatic ether present in the oxazine ring were observed as sharp peaks at 1045 cm^{-1} and 1213 cm^{-1} respectively. The -CH_2-N-Ar present in the oxazine ring was confirmed by the appearance of a stretching peak at 1121 cm^{-1}. The trisubstitited benzene ring shows characteristic sharp peak at 1503 cm^{-1}. The aromatic C=C stretching vibrations were noted at 1602 cm^{-1}. The C≡N stretching peak present in THQ-ca was noted at 2214 cm^{-1}. The stretching vibration of methyl groups were appeared in the range between 2850 and 2980 cm^{-1}.

The thermal ring opening polymerization of THQ benzoxazine resins was charecterised using FTIR technique. From the IR spectra, no peak was found at around 942 cm^{-1} after the thermal curing of THQ-BZ monomers (Fig. 3b). The intensities of C-O-C and C-N-C stretching vibrations were also reduced significanly after the polymerization (ROP) of monomers. A broad peak appeared at around for 3100 cm^{-1} was due to the presence of phenolic hydroxyl group which was formed after the cleavage of oxazine ring.

4.2. Curing behaviour

The DSC thermogram of THQ based benzoxazine resins were shown in Fig. 4. The DSC analysis was carried out at the rate of 10 °C/min under nitrogen environment. The DSC traces show exothermic peaks which reflects the release of heat energy during ROP of monomers. The exothermic peak maxima values show the exact temperature required for the benzoxazine monomers to undergo polymerization process. Most of the benzoxazine monomers show a single exothermic curing peak, unless there is a presence of cross-linkable group other than oxazine. However, in the case of THQ-BZ monomers, a double curing pattern was noticed from the DSC curves. The two curing peaks were emerged closely to each other. The occurance of two curing peaks may be due to the presence of oxazine rings at two different environments (Fig. 4). The oxazine ring ‘a’ in the THQ-BZ monomer was formed next to the tert-butyl group while the oxazine ring ‘b’ was formed away from the tert-butyl group due to steric hinderance caused by the bulky tert-butyl group. The electron donating nature (+I effect) of the tert-butyl group leads to faster curing of the oxazine ring ‘a’ at slightly lower temperature than that of the oxazine ring ‘b’. Other than THQ-ea and THQ-ca, the four THQ-BZ shows two distinct narrow curing peaks. In the case of THQ-ea and THQ-ca, the ethynyl group and cyanide group present in the amines may tends to thermally cross-link which are also exothermic processes. These exothermic cross-linking of ethynyl and cyanide groups gets overlapped with the curing peak of oxazine rings, which leads to the appearance of quite broad curing peaks. The curing onset, offset and exothermic peak temperatures of the THQ-BZ monomers are presented in Table 1.

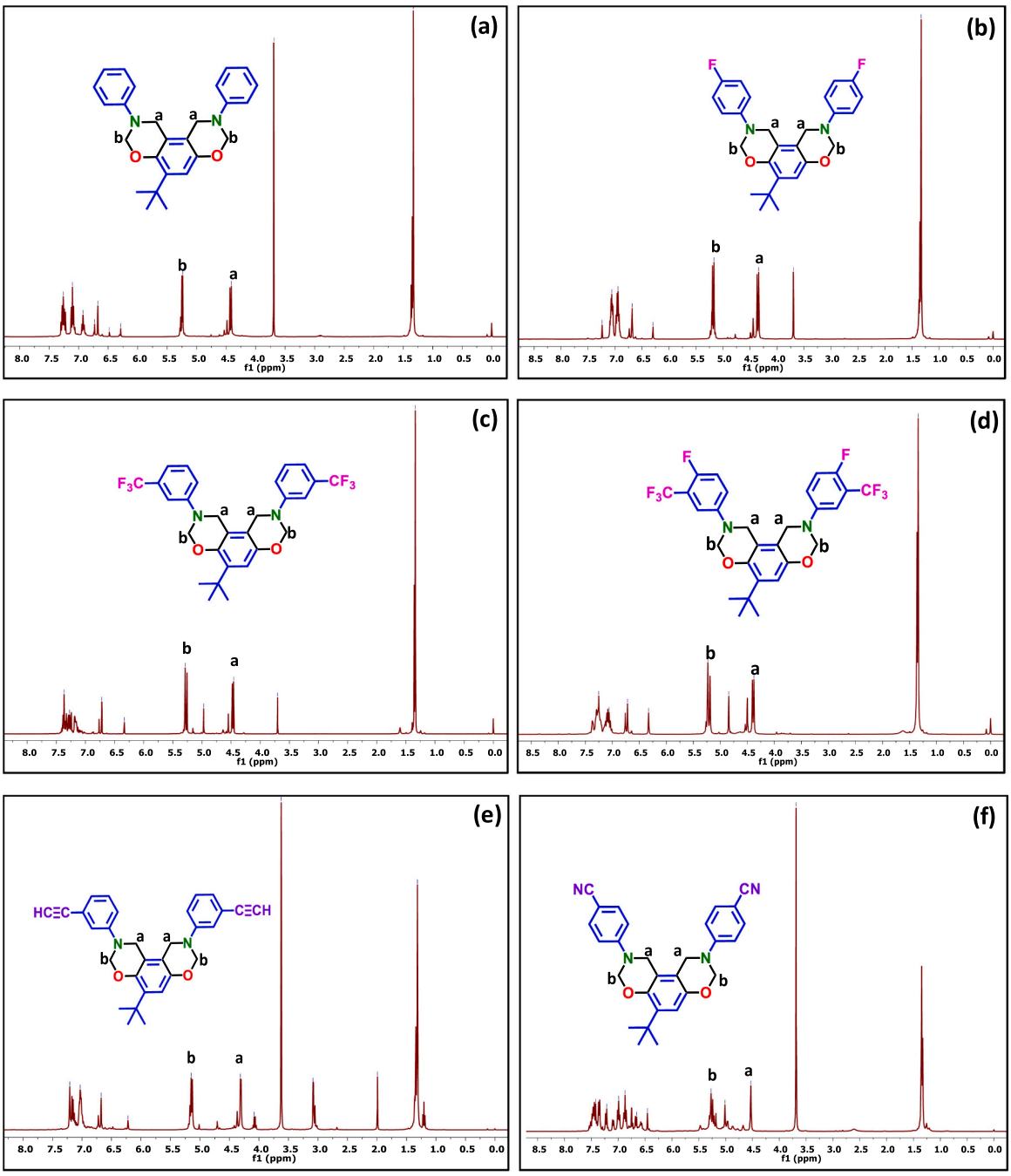

Fig. 1. ^{1}H NMR spectra of (a) THQ-a, THQ-fa, (b) THQ-tfma, (c) THQ-4ftma, (d) THQ-ea and (e) THQ-ca.

4.3. Thermal behaviour

The thermal stability of THQ based polybenzoxazines were studied using TGA technique at the heating of 20 °C/min under N_2 atmosphere (Fig. 5). There are three steps occurred in the thermal degradation of polybenzoxazines: 1. cleavage of terminal amines, 2. Decomposition of internal amines groups in the cross linked chain, and 3. breaking of Mannich link in the polymer chain. Final step is responsible for the maximum degradation of the polybenzoxazine. All the three steps occur simultaneously and gives a single degradation curve. From the degradation curve, the maximum temperature required for polybenzoxazine degradation can be obtained and it is denoted as T_{max}. The thermal stability of the synthesized polybenzoxazines were often discussed in terms of T_{max} and char residue values. The THQ-PBZ showed excellent thermal stability with char yield values above 40 % and T_{max} values above 470 °C (Fig. 5). This is because of the rich aromatic content present in the amine moieties, which gets cross-linked to form a three dimensional network structure. While comparing the six THQ-PBZ, the THQ-ca and THQ-ea show better thermal stability with higher char yield values of 60 % and 57 % respectively than those of other samples. This is due to the additional crosslinking of C≡C and C≡N to form a six membered benzene like structure during polymerization. The temperature at which the occurrence of 5 % weight loss (Td 5 %), 10 % weight loss (Td10 %), and maximum degradation (Td), char yield (%) and calculated limiting oxygen index (LOI) values of the THQ-PBZ are presented in Table 2.

4.4. Hydrophobic behaviour

The hydrophobic behaviour of the THQ-PBZ was studied using

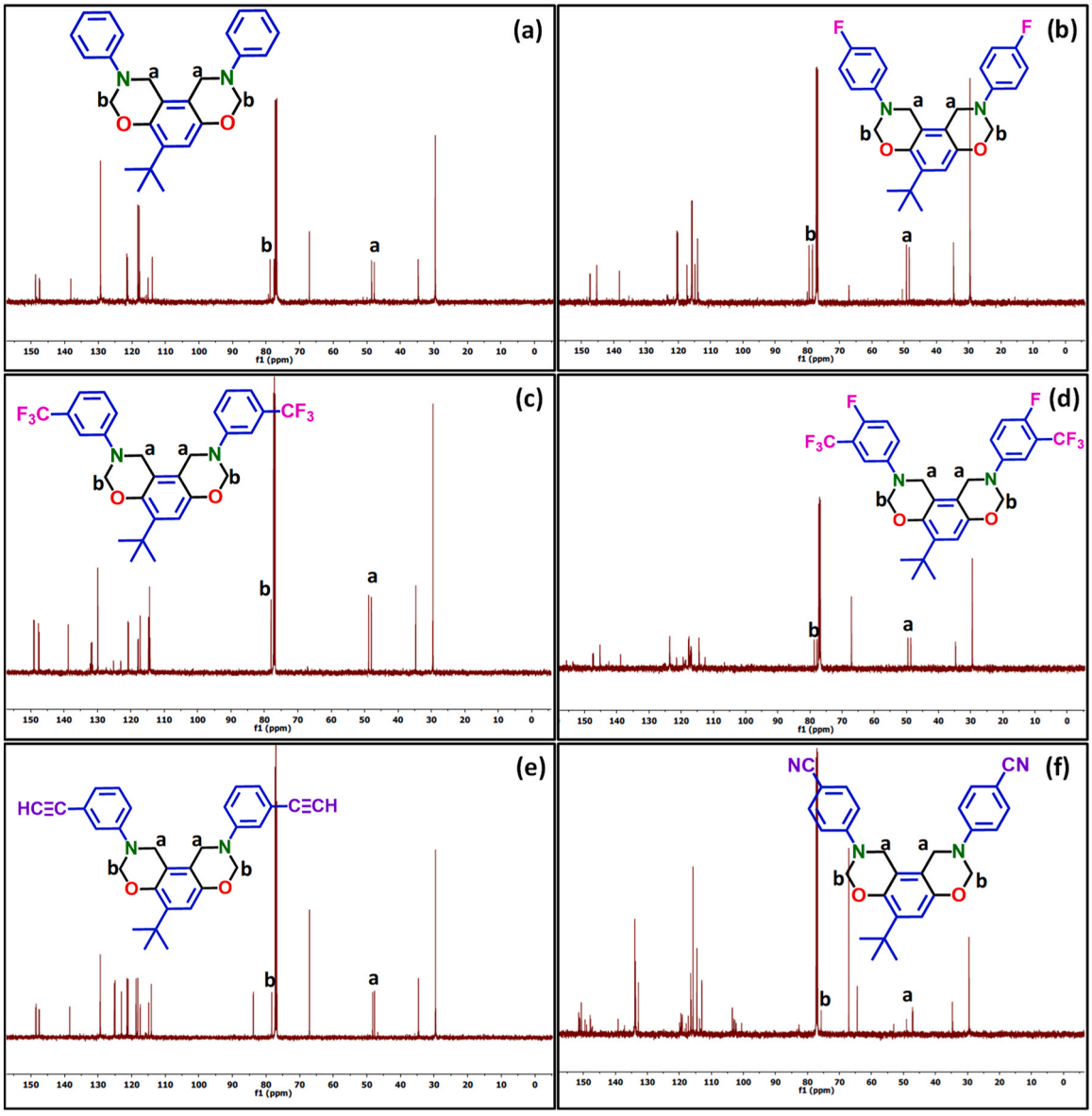

Fig. 2. ^{13}C NMR spectra of (a) THQ-a, (b) THQ-fa, (c) THQ-tfma, (d) THQ-4ftma, (e) THQ-ea and (f) THQ-ca.

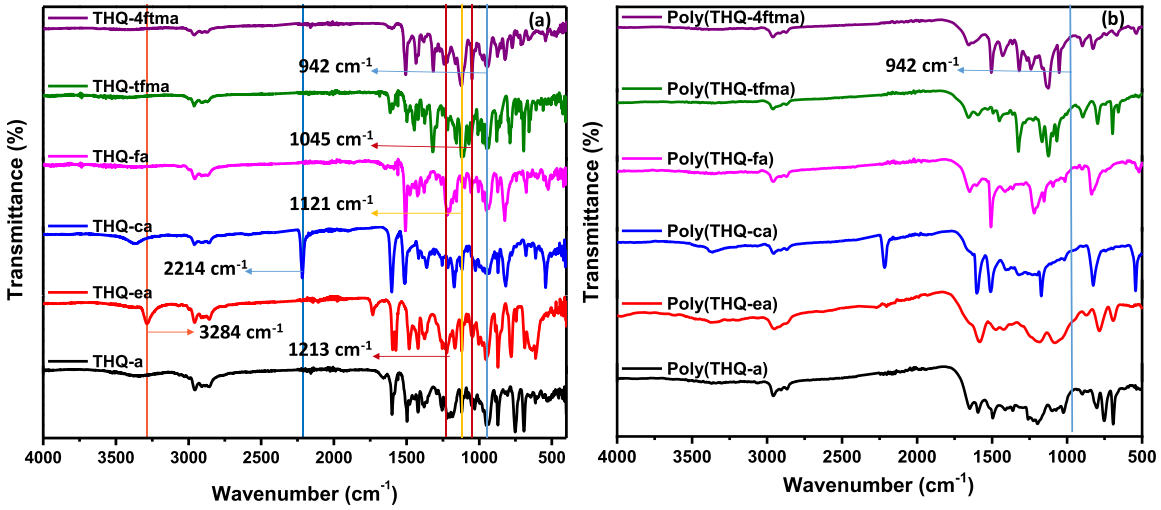

Fig. 3. FTIR spectra of (a) THQ-BZ monomers and (b) THQ-PBZ polymers.

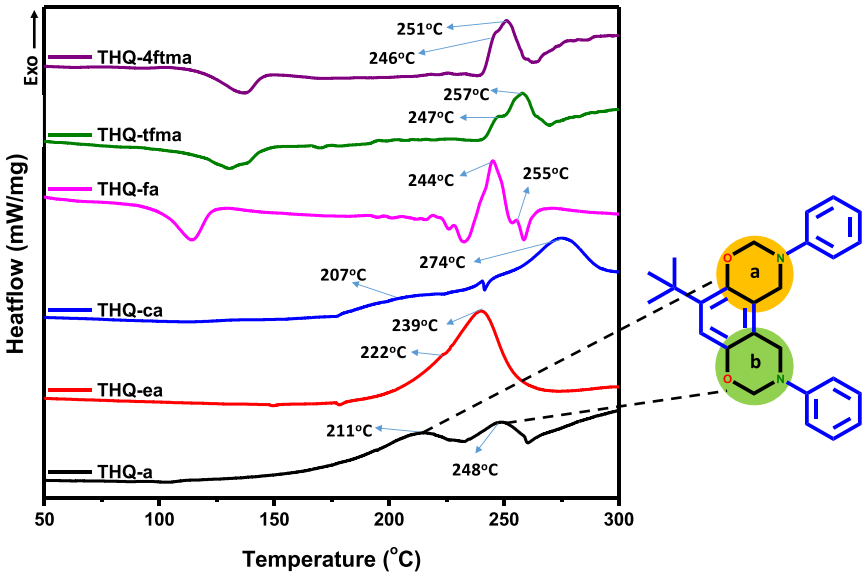

Fig. 4. DSC thermogram of THQ-BZ.

Table 1
Curing behaviour of THQ-BZ monomers.

THQ based benzoxazines	T_i (C)	T_p (C)	T_f (C)
THQ-a	160	211, 248	264
THQ-ea	181	222, 239	277
THQ-ca	169	207, 274	298
THQ-fa	214	244, 255	268
THQ-tfma	232	247, 257	273
THQ−4ftma	231	246, 251	269

Kyowa goniometer with water as probe liquid. The uneven surface of the polybenzoxazines were converted into even surface using sanding machin. The THQ-PBZ showed good water repelling property with water contact angle values above 144°. The value of higher water contact angle of PBZ was observed, due to the roughness of the surface and tert-butyl group substitution in hydroquinone. Also the presence of fluorine in the amine moieties of poly(THQ-fa), poly(THQ-tfma) and poly(THQ-4ftma) leads to higher moisture resistance property with enhanced values of water contact angle of around 150°. The roughness of the surface, covalent nature of polybenzoxazine provides higher surface free

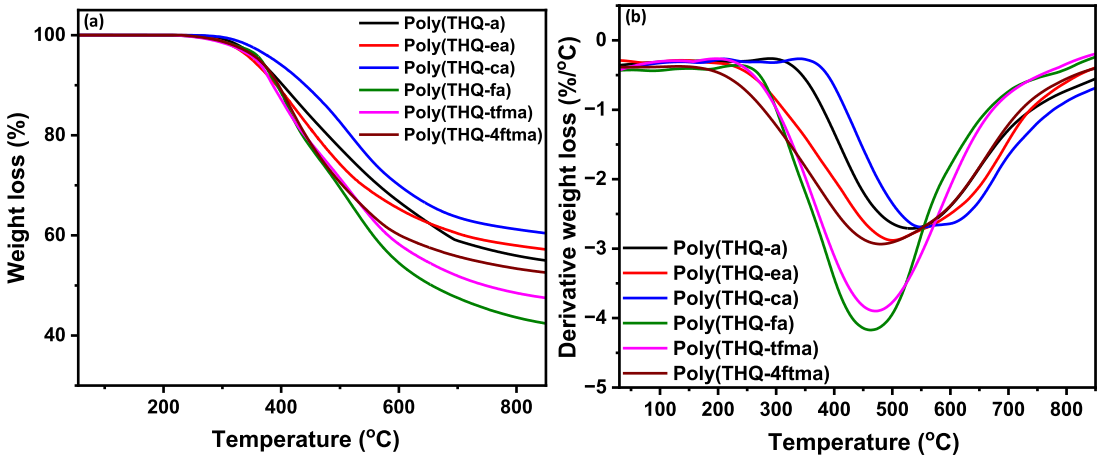

Fig. 5. (a) TGA curves and (b) DTG plots of THQ-PBZ.

Table 2
Thermal stability of tertiary butyl hydroquinone based polybenzoxazine.

Sample name	5 % weight loss (°C)	10 % weight loss (°C)	Maximum degradation (°C)	Char yield % at 850°C	LOI*	WCA (± 2°)
Poly(THQ-a)	361	403	522	55	39	147
Poly(THQ-ea)	353	391	492	57	40	146
Poly(THQ-ca)	388	440	553	60	41	144
Poly(THQ-fa)	366	393	470	42	34	149
Poly(THQ-tfma)	358	385	473	48	36	151
Poly(THQ−4ftma)	363	395	474	53	38	152

* Calculated by van Krevelen and Hoftyzer equation

energy, which helps to get higher water contact angle. Similarly, the hydrophobic behavior of the THQ-PBZ coated MS plates have been studied and the water contact angle values obtained are ~100°. The coating surfaces are very smooth hence a lower contact angle has been obtained. Yet the values are higher than 90°, which is fairly hydrophobic in nature. Because of the smooth surface the water droplet gets flattened on the surface of the coated MS plates but no penetration of water droplet is noted (Fig. S1). The water contact angle images and the values of the THQ-PBZ are presented in Fig. 6 and Table 2.

4.5. Adhesion property of the coating

The adhesion of the THQ-PBZ coating on the metal substrate was tested using crosscut analysis. A knife was used to create small squares on the surface of the coatings ensuring the angle between two lines is right angle. After creating the grid, the coating was genly wiped using cotton. Then a piece of adhesive tape was made to stick into the grid and then rapidly pull off from the surface. The adhesive tape pulling has been repeated for 5 times with new piece of tape for each time. There is no square of coating has been flaked off or removed during the entire test (Fig. 7). This shows the excellent adhesion nature of the coating to the metal substrate.

4.6. Corrosion resistance property

The corrosion resistance property of the THQ-PBZ has been studied using potentio-dynamic polarization curves and electrochemical impedance spectroscopy. The anti-corrosion behaviour of the THQ-PBZ coated MS specimen were tested in 3.5 % NaCl solution at room temperature. Using the Tafel extrapolation method, the corrosion current density (I_{corr}), corrosion potential (E_{corr}) were obtained (Fig. 8). The anodic and cathodic current densities (I_{corr}) of the THQ-PBZ coated MS specimen have been decreased effectively when compared to that of uncoated (bare) MS. This indicates that the THQ-PBZ act as a barrier for the electrochemical reactions to take place and very minimum electric current is passing through the surface of the MS. The corrosion potential (E_{corr}) of the coated MS plates were increased through a positive shift, which indicates that a higher potential is required for the electrochemical corrosion reaction to occur. From the corrosion current density, the corrosion protection efficiency (η_p) and the rate of corrosion (CR) can be calculated using the Eqs. (1) and (2) respectively,

$$\text{Corrosion protection efficiency } (\eta_p),\ \% = [(I_{corr}^{\circ} - I_{corr}) / I_{corr}^{\circ}] \times 100 \quad \ldots\ldots \quad (1)$$

$$\text{Rate of corrosion (CR)} = MI_{corr} / \rho nF \quad \ldots\ldots \quad (2)$$

where I_{corr}° and I_{corr} are the corrosion current densities of uncoated (bare) MS plate and THQ-PBZ coated MS plates respectively, M is the molecular mass of ferrum (55.85 g/mol), ρ is the density of mild steel (7.8 g/cm^3), n is the number of electrons transferred (n = 2) and F is the Faraday's constant (96500 A s /mol).

From the Tafel curves, the anodic (β_a) and cathodic (β_c) slopes can also be determined. The anodic and cathodic slopes determines the activation energy required for the electrochemical reaction to takes place. A positive or higher slope value indicates the higher amount of activation energy required for the corrosion reaction to occur. The values of I_{corr}, E_{corr}, β_a, β_c, CR and η_p %, which are derived from the Tafel curves are presented in Table 3. Among all the THQ-PBZ coated MS plates, the poly(THQ-4ftma) shows the lowest corrosion current density of 1.94×10^{-11} mA, with high corrosion potential of 0.554 mV, indicating the excellent corrosion resistance behaviour of the coating. The THQ-PBZ coated MS specimen shows the corrosion protection efficiency above 99 %. Among the coated MS specimens, the poly(THQ-4ftma) coated MS shows better corrosion protection efficiency with very minimum corrosion rate of 2.66×10^{-5} mm/year. The corrosion rates and the value of water contact angle of the of the synthesized THQ-PBZ are inter related to each other. The highly hydrophobic polybenzoxazines possess very low corrosion rate (Fig. 9). This is because the hydrophobic nature of the THQ-PBZ restricts the marine solution to penetrate into the surface of the mild steel, thus leading to very much low corrosion rates. The poly(THQ-4ftma) being higly hydrophobic which prevents the electrochemical corrosion reaction to takes place quickly.

The electrochemical behaviour of the uncoated and THQ-PBZ coated MS specimens has been further studied by EIS using equivalent electrical circuit model which is required to fit all the data obtained from the Nyquist plot. Different data can be obtained from the capacitive loop of the Nyquist plots such as solution resistance (R_s), charge transfer resistance offered by the coating (R_{ct}), electrical double layer capacitance (C_{dl}), constant phase elements (CPE) such as Q and 'n' which are magnitude and a component used to describe the roughness of the

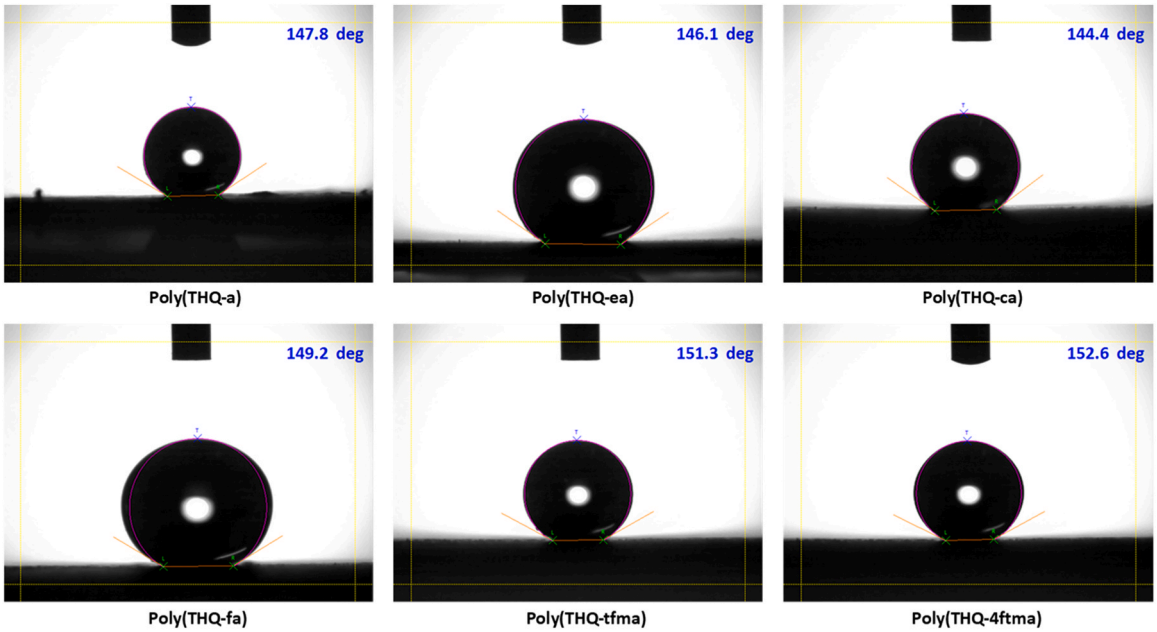

Fig. 6. Water contact angle of THQ-PBZ.

Fig. 7. Crosscut test of THQ-PBZ coated MS plate.

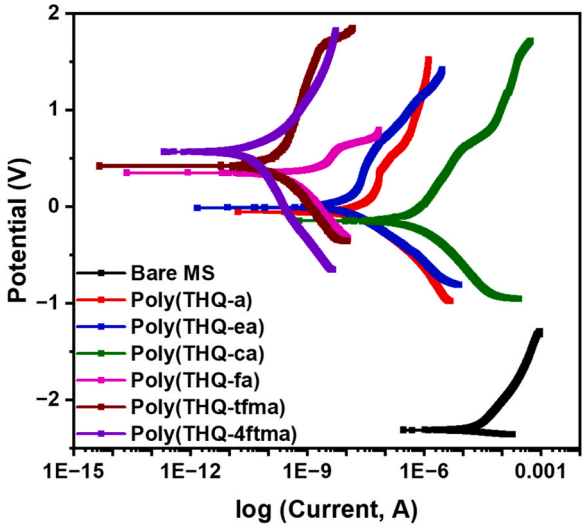

Fig. 8. Tafel curves of bare MS and THQ-PBZ coated MS.

surface respectively (Fig. 10). The R_s value indicates the resistance offered by the electrolyte solution and the R_{ct} value determines the resistance offered by the polybenzoxazine coating on the surface. The higher R_{ct} value of the THQ-PBZ coated MS plates indicate the higher resistance of the coating towards electrochemical reaction to occur. From the R_{ct} value of uncoated and coated MS specimens, the corrosion protection efficiency can be calculated using the Eq. (3),

$$\eta_i\ (\%) = (R_{ct} - R_{ct}^{\circ} / R_{ct}) \times 100 \ldots\ldots\ldots \quad (3)$$

where R_{ct}° and R_{ct} are the charge transfer resistance of the uncoated (bare) and THQ-PBZ coated MS specimens respectively. The corrosion protection efficiency of the THQ-PBZ coated MS specimen calculated from the EIS data (η_i) are in accordance with the efficiency calculated using Tafel data (η_p).

The electrical double layer capacitance (C_{dl}) value defines the amount of electrical energy can be stored on the interface formed between the solution and the polybenzoxazine coating on the surface of the metal plates. A higher C_{dl} indicates that the stored charge can pass through the interfacial layer and tends to interact with the metal surface. For a better anti-corrosive coating, the C_{dl} value must be lower than that of the uncoated metal. The value of C_{dl} can be calculated with the CPE magnitude Q and 'n' values using the Eq. (4),

$$C_{dl} = Q\ (\omega_{max})^{n-1} \ldots\ldots \quad (4)$$

where ω is the angular frequency in rad S^{-1}, which can be calculated from $\omega = 2\pi f_{max}$, where f_{max} is the maximum frequency. The calculated values of C_{dl} for the THQ-PBZ coated MS specimen are lower than that of the C_{dl} value of uncoated MS plate. This ascertains that the polybenzoxazine coating effectively reduces the capacitance behaviour of the interface formed on the metal surface.

Among the THQ-PBZ coated MS plates, the poly(THQ-4ftma) coated MS specimen shows the highest R_{ct} value of $1.94 \times 10^7\ \Omega\ cm^2$, which is higher than that of the uncoated MS plate. Also the corrosion protection efficiency (η_i) calculated from the EIS data shows that the poly(THQ-4ftma) coated MS specimen exhibits better corrosion resistance property than that of the other THQ-PBZ coated MS plates and act as an

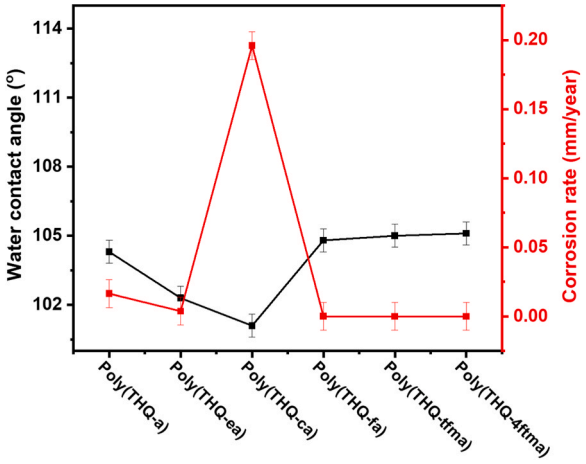

Fig. 9. Relationship between hydrophobicity and corrosion rate of the THQ-PBZ coated MS plates.

Table 3
Potentiodynamic polarization parameters obtained from Tafel plots of bare MS and THQ-PBZ coated MS.

THQ-PBZ Coated MS	I_{corr} (mA)	E_{corr} (mV)	β_a (mV dec^{-1})	β_c (mV dec^{-1})	CR (mm $year^{-1}$)	η_p (%)
Bare MS	3.21×10^{-5}	−2.310	−2.379	−2.278	4.41×10^{1}	-
Poly(THQ-a)	1.20×10^{-8}	−0.053	−0.413	0.303	1.65×10^{-2}	99.96
Poly(THQ-ea)	2.78×10^{-9}	0.009	−0.210	0.275	3.82×10^{-3}	99.99
Poly(THQ-ca)	1.43×10^{-7}	−0.143	−0.384	0.081	1.96×10^{-1}	99.55
Poly(THQ-fa)	7.21×10^{-11}	0.334	0.263	0.459	9.90×10^{-5}	99.99
Poly(THQ-tfma)	2.73×10^{-11}	0.422	0.124	0.731	3.75×10^{-5}	99.99
Poly(THQ−4ftma)	1.94×10^{-11}	0.554	0.287	0.945	2.66×10^{-5}	99.99

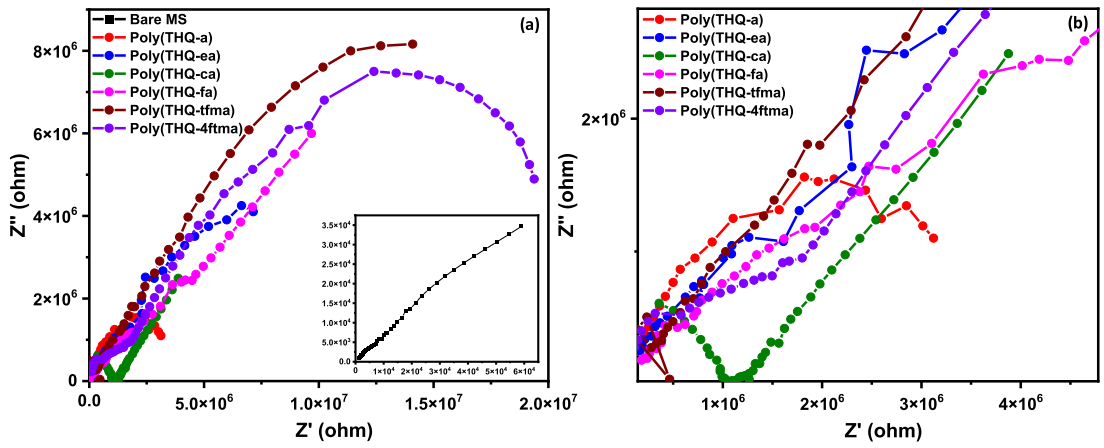

Fig. 10. (a) and (b) Nyquist plots of bare MS and THQ-PBZ coated MS.

effective barrier towards electrochemical reactions. This is because of the presence of fluorine atoms which resists the electric charges in the solution to attack the surface of the mild steel. The data obtained from the Nyquist plots have been given in Table 4.

4.7. Anti-microbial activity

The antimicrobial activity of the synthesized THQ-BZ are presented in Fig. 11 and Fig. S2. The anti-microbial activity of the tert-butyl hydroquinone was reported in earlier studies. The good bactericidal property of the tert-butyl hydroquinone is mainly due to the phenolic –OH group present in it. Surprisingly in the case of THQ-BZ, the monomers show significant inhibition towards the growth of bacteria even with the phenolic group occupied. This may be due to the presence of free methyl groups in tert-butyl moiety. For the assessment of anti-bacterial activity different type of gram positive bacteria (*S. aureus*) and gram negative bacteria (*E.coli*) were selected. All the THQ-BZ shows better activity against gram positive bacteria (*S. aureus*) with inhibition zones more than 20 mm. Whereas, the activity against the *E.coli* was quite low when compared to that of *S.aureus*. Because the gram negative bacteria have a outer membrane made up of lipopolysaccharides that surrounds the peptidoglycan cell wall. The tert-butyl hydroquinone itself cannot be able to penerate this outer membrane effectively, which leads to the limited activity against gram negative bacteria. Indeed, with the help of an outer membrane penetrating agent, the THQ-BZ can be able to disrupt the outer membrane as well as cell wall of the gram negative bacteria. Among the THQ-BZ, the THQ-ca shows the highest inhibition zone of 32 mm for *S. aureus* and 20 mm for *E.coli*. E9ven-though all the THQ-BZ shows limited activity against gram negative bacteria, the THQ-ca displays a better inhibition zone of 20 mm against *E.coli*. This is due to the presence of both polar -C≡N and non polar tert-butyl groups present in the THQ-ca which makes the compound slightly amphiphilic in nature. This polar -C≡N can able to destroy the outer membrane as well as the inner cell wall and leads to the damage of bacterial cells. This disruption of bacterial cells leads to the limited growth of bacteria within the range of action. The images of petri plates representing the zone of inhibition of THQ-BZ are given in Fig. S2 and the inhibition zone diameters are given in Table 5.

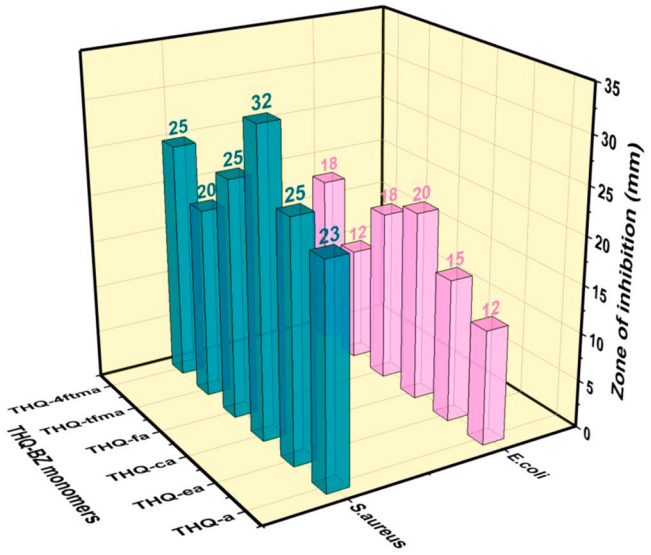

Fig. 11. Inhibition zones of THQ-BZ.

5. Conclusion

The bifunctional benzoxazines were prepared using tertiary butyl hydroquinone with different amines (aniline, fluoro aniline, trifluoro methyl aniline, 4-fluoro trifluoro methyl aniline, ethynyl aniline, cyano aniline) and paraformaldehyde. The structure of prepared benzoxazine resins was elucidated by FTIR and ^{1}H NMR spectral analyses.The curing temperature of (THQ-a, THQ-fa, THQ-tfma, THQ-4ftfma, THQ-ea, THQ-

Table 4
Electrochemical impedance spectroscopy parameters obtained from Nyquist plots of bare MS and THQ-PBZ coated MS.

THQ-PBZ Coated MS	R_s (Ω cm^2)	R_{ct} (Ω cm^2)	Q_{dl} ($\Omega^{-1}s^n cm^{-2}$)	n	C_{dl} (μF cm^{-2})	η_i (%)
Bare MS	1346	5.90×10^4	9.42×10^{-4}	0.791	93.60	-
Poly(THQ-a)	2508	3.12×10^6	5.84×10^{-5}	0.875	14.69	98.10
Poly(THQ-ea)	3710	7.14×10^6	3.90×10^{-5}	0.869	9.17	99.17
Poly(THQ-ca)	3586	3.88×10^6	4.65×10^{-5}	0.886	13.20	98.47
Poly(THQ-fa)	9310	9.68×10^6	3.33×10^{-5}	0.856	6.78	99.39
Poly(THQ-tfma)	1542	1.41×10^7	2.80×10^{-5}	0.871	6.72	99.58
Poly(THQ−4ftma)	9098	1.94×10^7	1.84×10^{-5}	0.878	4.78	99.69

Table 5
Inhibition zones of THQ-BZ.

THQ-BZ Sample (1 mg/ml)	Zone of inhibition (mm)	
	Staphylococcus aureus	*Escherichia coli*
THQ-a	23	12
THQ-ea	25	15
THQ-ca	32	20
THQ-fa	25	18
THQ-tfma	20	12
THQ−4ftma	25	18

ca) benzoxazines was studied using DSC technique. From the TGA analysis, the poly(THQ-ca) posessess higher value of char yield (60 %) and the value of higher degradation temperature (553 °C) than other polybenzoxazines. From the water contact angle studies, the poly(THQ-4ftma) possess better water resisting behavior (WCA 152°) than that of other polybenzoxazines.The THQ-PBZ were coated on the surfaces of mild steel and the corrosion resistance property of the coated MS specimens were studied. The potentiostatic dynamic polarization results of the THQ-PBZ coated MS specimens show 99.99 % corrosion protection efficiency than that of the uncoated MS specimen. The poly(THQ-4ftma) shows better corrosion protection than that of other THQ-PBZ because of its higher hydrophobicity. The THQ-BZ were tested for their activity against the growth of *S.aureus* and *E.coli* bacteria. The THQ-ca shows effective inhibition towards the growth of both the bacteria with inhibition zone of 32 mm and 20 mm respectively. Data obtained from thermal, hydrophobic, corrosion and microbial studies suggest that the THQ based polyenzoxazines can be efficiently utilized as high performance corrosion resistant and anti-bacterial coatings under moist and thermal environments.

Declaration of Competing Interest

The authors declare that they have no known competing financial interests or personal relationships that could have appeared to influence the work reported in this paper.

Appendix A. Supporting information

Supplementary data associated with this article can be found in the online version at doi:10.1016/j.nxmate.2025.100723.

References

[1] P.A. Sørensen, S. Kiil, K. Dam-Johansen, C.E. Weinell, Anticorrosive coatings: a review, J. Coat. Technol. Res. 6 (2009) 135–176, https://doi.org/10.1007/s11998-008-9144-2.

[2] H. Huang, X. Sheng, Y. Tian, L. Zhang, Y. Chen, X. Zhang, Two-dimensional nanomaterials for anticorrosive polymeric coatings: a review, Ind. Eng. Chem. Res. 59 (2020) 15424–15446, https://doi.org/10.1021/acs.iecr.0c02876.

[3] T. Peng, R. Xiao, Z. Rong, H. Liu, Q. Hu, S. Wang, X. Li, J. Zhang, Polymer nanocomposite-based coatings for corrosion protection, Chem. Asian J. 15 (2020) 3915–3941, https://doi.org/10.1002/asia.202000943.

[4] H. Xu, Y. Zhang, A review on conducting polymers and nanopolymer composite coatings for steel corrosion protection, Coatings 9 (2019) 807, https://doi.org/10.3390/coatings9120807.

[5] W. Yuan, D. Xia, S. Wu, Y. Zheng, Z. Guan, J.V. Rau, A review on current research status of the surface modification of Zn-based biodegradable metals, Bioact. Mater. 7 (2022) 192–216, https://doi.org/10.1016/j.bioactmat.2021.05.018.

[6] M. Zhang, H. Wang, T. Nie, J. Bai, F. Zhao, S. Ma, Enhancement of barrier and anti-corrosive performance of zinc-rich epoxy coatings using nano-silica/graphene oxide hybrid, Corros. Rev. 38 (2020) 497–513, https://doi.org/10.1515/corrrev-2020-0034.

[7] M.M. K, H. Arumugam, B. Krishnasamy, A. Muthukaruppan, Sesamol-Based Polybenzoxazines for Ultra-Low-k, High-k and Hydrophobic Coating Applications, (2023). ⟨https://doi.org/10.1039/d3nj00531c⟩.

[8] H. Srinivasan, J. Krishnan, Structure, Thermal, Hydrophobic, and Dielectric Properties of Bermuda Grass Ash Bio-silica, SBA-15, and rGO-Reinforced Bisphenol-BA-Based Polybenzoxazine Composites, (2023) 1–20. https://doi.org/10.1002/app.54447.

[9] Y. Lyu, H. Ishida, Natural-sourced benzoxazine resins, homopolymers, blends and composites: a review of their synthesis, manufacturing and applications, Prog. Polym. Sci. 99 (2019) 101168, https://doi.org/10.1016/j.progpolymsci.2019.101168.

[10] S. Ranganathan, H. Arumugam, B. Krishnasamy, S. Sathy Srikandan, K. Mallaiya, M. Alagar, Bio-based polybenzoxazines as an efficient coatings to protect mild steel surfaces from corrosion, High. Perform. Polym. 34 (2022) 593–603, https://doi.org/10.1177/09540083221085163.

[11] A. Hariharan, P. Prabunathan, A. Kumaravel, M. Manoj, M. Alagar, Bio-based polybenzoxazine composites for oil-water separation, sound absorption and corrosion resistance applications, Polym. Test. 86 (2020) 106443, https://doi.org/10.1016/j.polymertesting.2020.106443.

[12] Y. Deng, L. Xia, G.L. Song, Y. Zhao, Y. Zhang, Y. Xu, D. Zheng, Development of a curcumin-based antifouling and anticorrosion sustainable polybenzoxazine resin composite coating, Compos. Part B Eng. 225 (2021) 109263, https://doi.org/10.1016/j.compositesb.2021.109263.

[13] C. Zhou, X. Lu, Z. Xin, J. Liu, Corrosion resistance of novel silane-functional polybenzoxazine coating on steel, Corros. Sci. 70 (2013) 145–151, https://doi.org/10.1016/j.corsci.2013.01.023.

[14] L. Wang, M. Yuan, Y. Zhao, Z. Guo, X. Lu, Z. Xin, Fabrication of superhydrophobic bio-based polybenzoxazine/hexagonal boron nitride composite coating for corrosion protection, Prog. Org. Coat. 167 (2022) 106863, https://doi.org/10.1016/j.porgcoat.2022.106863.

[15] J. Huang, C. Lou, D. Xu, X. Lu, Z. Xin, C. Zhou, Cardanol-based polybenzoxazine superhydrophobic coating with improved corrosion resistance on mild steel, Prog. Org. Coat. 136 (2019) 105191, https://doi.org/10.1016/j.porgcoat.2019.06.037.

[16] Y. Cao, C. Chen, X. Lu, D. Xu, J. Huang, Z. Xin, Bio-based polybenzoxazine superhydrophobic coating with active corrosion resistance for carbon steel protection, Surf. Coat. Technol. 405 (2021) 126569, https://doi.org/10.1016/j.surfcoat.2020.126569.

[17] G.A. Phalak, D.M. Patil, S.T. Mhaske, Synthesis and characterization of thermally curable Guaiacol based poly (benzoxazine –urethane) coating for corrosion protection on mild steel, Eur. Polym. J. (2016), https://doi.org/10.1016/j.eurpolymj.2016.12.030.

[18] A.M.M. Soliman, K.I. Aly, M.G. Mohamed, A.A. Amer, M.R. Belal, M. Abdel-Hakim, Synthesis, characterization and protective efficiency of novel polybenzoxazine precursor as an anticorrosive coating for mild steel, Sci. Rep. 13 (2023) 5581, https://doi.org/10.1038/s41598-023-30364-x.

[19] Q. Chen, L. Zhang, J. Zhang, S. Habib, G. Lu, J. Dai, X. Liu, Bio-based polybenzoxazines coatings for efficient marine antifouling, Prog. Org. Coat. 174 (2023) 107298, https://doi.org/10.1016/j.porgcoat.2022.107298.

[20] R. Bender, D. Féron, D. Mills, S. Ritter, R. Bäßler, D. Bettge, I. De Graeve, A. Dugstad, S. Grassini, T. Hack, M. Halama, E.H. Han, T. Harder, G. Hinds, J. Kittel, R. Krieg, C. Leygraf, L. Martinelli, A. Mol, D. Neff, J.O. Nilsson, I. Odnevall, S. Paterson, S. Paul, T. Prošek, M. Raupach, R.I. Revilla, F. Ropital, H. Schweigart, E. Szala, H. Terryn, J. Tidblad, S. Virtanen, P. Volovitch, D. Watkinson, M. Wilms, G. Winning, M. Zheludkevich, Corrosion challenges towards a sustainable society, Mater. Corros. 73 (2022) 1730–1751, https://doi.org/10.1002/maco.202213140.

[21] G. Latha, A. Hariharan, K. Balaji, A. Kumaravel, M. Alagar, Cardanol and bisphenol-F based benzoxazines with zirconium phosphate reinforced composites coating for protecting the mild steel surface from corrosion, J. Macromol. Sci. Part A Pure Appl. Chem. (2022) 1–13, https://doi.org/10.1080/10601325.2022.2118607.

[22] C.J. Raorane, T. Periyasamy, R. Haldhar, S.P. Asrafali, V. Raj, S.C. Kim, Synthesis of bio-based polybenzoxazine and its antibiofilm and anticorrosive activities, Materials 16 (2023), https://doi.org/10.3390/ma16062249.

[23] T. Periyasamy, S.P. Asrafali, C.J. Raorane, V. Raj, D. Shastri, S.-C. Kim, Sustainable chitosan/polybenzoxazine films: synergistically improved thermal, mechanical, and antimicrobial properties, Polymers 15 (2023), https://doi.org/10.3390/polym15041021.

[24] S. Sahu, R. Niranjan, R. Priyadarshini, B. Lochab, Benzoxazine-grafted-chitosan biopolymer films with inherent disulfide linkage: antimicrobial properties, Chemosphere 328 (2023) 138587, https://doi.org/10.1016/j.chemosphere.2023.138587.

[25] A. Khezerlou, A. pouya Akhlaghi, A.M. Alizadeh, P. Dehghan, P. Maleki, Alarming impact of the excessive use of tert-butylhydroquinone in food products: a narrative review, Toxicol. Rep. 9 (2022) 1066–1075, https://doi.org/10.1016/j.toxrep.2022.04.027.

[26] N. Ooi, I. Chopra, A. Eady, J. Cove, R. Bojar, A.J. O'Neil, Antibacterial activity and mode of action of tert-butylhydroquinone (tbhq) and its oxidation product, tert-butylbenzoquinone (tbbq), J. Antimicrob. Chemother. 68 (2013) 1297–1304, https://doi.org/10.1093/jac/dkt030.

[27] M. Raccach, E.C. Henningsen, Antibacterial effect of tertiary butylhydroquinone against two genera of gram positive Cocci, J. Food Sci. 47 (1982) 106–109, https://doi.org/10.1111/j.1365-2621.1982.tb11038.x.

[28] A. Raza, Y. Si, X. Wang, T. Ren, B. Ding, J. Yu, S.S. Al-Deyab, Novel fluorinated polybenzoxazine-silica films: chemical synthesis and superhydrophobicity, RSC Adv. 2 (2012) 12804–12811, https://doi.org/10.1039/c2ra21138f.

[29] P. Velez-Herrera, K. Doyama, H. Abe, H. Ishida, Synthesis and characterization of highly fluorinated polymer with the benzoxazine moiety in the main chain, Macromolecules 41 (2008) 9704–9714, https://doi.org/10.1021/ma801253a.

[30] K. Krishnadevi, S. Devaraju, S. Sriharshitha, M. Alagar, Y. Keerthi Priya, Environmentally sustainable rice husk ash reinforced cardanol based

polybenzoxazine bio-composites for insulation applications, Polym. Bull. (2019), https://doi.org/10.1007/s00289-019-02854-4.
[31] M.M. K, B. Krishnasamy, H. Arumugam, K. Saravana Mani, A. Muthukaruppan, Sustainable strategies for fully biobased polybenzoxazine composites from trifunctional thymol and biocarbons: advancements in high-dielectric and antibacterial corrosion implementations, ACS Sustain. Chem. Eng. 12 (2024) 2225–2240, https://doi.org/10.1021/acssuschemeng.3c06314.
[32] C. Zhou, S. Lin, Y. Wang, T. Zhao, Y. Tian, X. Gui, Impact of Ring-Closed Ratio on Properties of Benzoxazine via Solvent-Free Continuous Flow, (2025) 1–12. https://doi.org/10.1002/ceat.70002.